RESEARCH ARTICLE

Botany
American Journal of

How and why do species break a developmental trade-off? Elucidating the association of trichomes and stomata across species

Alec S. Baird[1,2] | Camila D. Medeiros[1] | Marissa A. Caringella[1] | Julia Bowers[1] | Michelle Hii[1] | John Liang[1] | Joshua Matsuda[1] | Kirthana Pisipati[1] | Caroline Pohl[1] | Benjamin Simon[1] | Silvard Tagaryan[1] | Thomas N. Buckley[3] | Lawren Sack[1]

[1]Department of Ecology and Evolutionary Biology, University of California Los Angeles, 621 Charles E. Young Drive South, Los Angeles, CA 90095, USA

[2]Institute of Plant Sciences, University of Bern, Altenbergrain 21, Bern 3013, Switzerland

[3]Department of Plant Sciences, University of California, Davis, One Shields Avenue, Davis, CA 95616, USA

Correspondence

Alec S. Baird, Department of Ecology and Evolutionary Biology, University of California Los Angeles, 621 Charles E. Young Drive South, Los Angeles, CA 90095 USA.
Email: alecsbaird@gmail.com

Abstract

Premise: Previous studies have suggested a trade-off between trichome density (D_t) and stomatal density (D_s) due to shared cell precursors. We clarified how, when, and why this developmental trade-off may be overcome across species.

Methods: We derived equations to determine the developmental basis for D_t and D_s in trichome and stomatal indices (i_t and i_s) and the sizes of epidermal pavement cells (e), trichome bases (t), and stomata (s) and quantified the importance of these determinants of D_t and D_s for 78 California species. We compiled 17 previous studies of D_t–D_s relationships to determine the commonness of D_t–D_s associations. We modeled the consequences of different D_t–D_s associations for plant carbon balance.

Results: Our analyses showed that higher D_t was determined by higher i_t and lower e, and higher D_s by higher i_s and lower e. Across California species, positive D_t–D_s coordination arose due to i_t–i_s coordination and impacts of the variation in e. A D_t–D_s trade-off was found in only 30% of studies. Heuristic modeling showed that species sets would have the highest carbon balance with a positive or negative relationship or decoupling of D_t and D_s, depending on environmental conditions.

Conclusions: Shared precursor cells of trichomes and stomata do not limit higher numbers of both cell types or drive a general D_t–D_s trade-off across species. This developmental flexibility across diverse species enables different D_t–D_s associations according to environmental pressures. Developmental trait analysis can clarify how contrasting trait associations would arise within and across species.

KEYWORDS

Adaptation, California, cell size, development, functional traits, physiology

Trichomes, plant hairs, have fascinated botanists for centuries (Figure 1; Haberlandt, 1914; Werker, 2000; Evert, 2006) due to their diversity in number, shape, size, and adaptive functions and occurrence in the majority of plant species (Evert, 2006). Trichomes can be uni- or multicellular, with straight, spiral, star, hooked or branched morphology, and they can be glandular (Werker, 2000; Li et al., 2023). Trichome morphology and number differ among organs on the same plant,

between surfaces of the same organ, in plastic responses to environmental stress, and among species (Bickford, 2016; Wang et al., 2021). The leaf trichome density (D_t, Table 1), i.e., the number of trichomes per leaf area, influences plant performance in crop and wild ecosystems, depending on trichome properties and their environmental context (Doughty et al., 2011; Snyder and Antonious, 2011; Bickford, 2016; Huchelmann et al., 2017; Sack and Buckley, 2020; Gupt
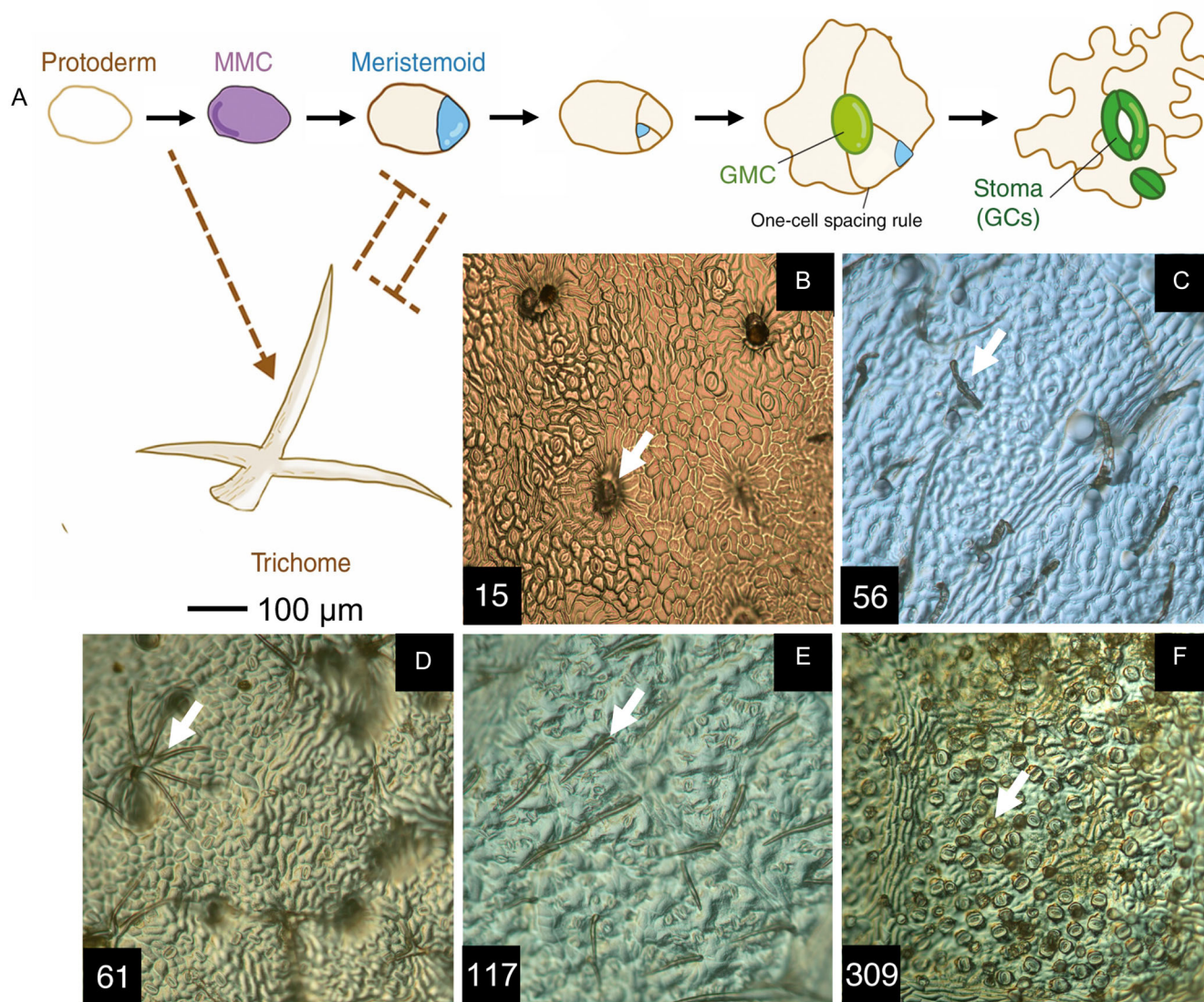
FIGURE 1   Developmental sequence of leaf trichome and stomata formation and diversity of leaf trichomes of California species. (A) Developmental sequence of trichome and stomatal formation (modified from Figures 2 and 3 of Torii, 2021). In eudicots, trichomes are initiated by protodermal cells or meristemoid mother cells (MMC), i.e., before stomatal meristemoid formation. Asymmetric cell divisions of the MMC result in meristemoid precursors that divide further and then differentiate into guard mother cells (GMC), which divide and differentiate into stomatal guard cells (GC). High activity of SPEECHLESS (SPCH) proteins in the protoderm and MMCs drives stomatal formation. SPCH activity is also high in meristemoid cells and drives upregulation of TOO MANY MOUTHS (*TMM*), which contributes to ensuring one-cell spacing and also reduces trichome numbers via an unknown mechanism. SPCH activity also leads to the upregulation of genes that drive trichome formation. Both trichome and stomatal precursors may exclude each other's development from protodermal precursors. Abaxial trichomes visualized from nail varnish peels of leaf surfaces for (B) *Ericameria cuneata*, (C) *Encelia californica*, (D) *Quercus garryana*, (E) *Ceanothus cordulatus*, and (F) *Chrysolepis sempervirens*. The white arrow in panels (B–F) indicates a trichome; the number at the bottom left indicates the abaxial trichome density (D_t) for that species, ordered from lowest to highest.

et al., 2021; Vinod et al., 2023). A high D_t reduces the absorbance of light, including UV, and would in principle contribute a thicker boundary layer (Ehleringer et al., 1976; Ehleringer and Björkman, 1978), and thereby lessen leaf overheating and photochemical damage, enabling gain in carbon accumulation at lower transpiration rates, improving water-use efficiency, an advantage in hot and arid environments (Ehleringer and Mooney, 1978; Ripley et al., 1999; Bickford, 2016). A high D_t may also reduce surface wettability during rainy conditions (Brewer et al., 1991) and/or improve water uptake (Fernández et al., 2014; Kim et al., 2017;

Schwerbrock and Leuschner, 2017; Schreel et al., 2020; Pan et al., 2021; Li et al., 2023). In many species, trichomes are important for sequestering and detoxifying metals (Choi et al., 2001; Azmat et al., 2009; Li et al., 2023). Lastly, higher D_t may increase resistance to herbivores and pathogens by providing a physical barrier and/or influencing secondary metabolite production (Agren and Schemske, 1993; Mauricio, 1998; Valverde et al., 2001; Hare and Elle, 2002; Handley et al., 2005; Agrawal et al., 2009).

The key importance of stomata, which strongly determine plant gas exchange rates (Wong et al., 1979;

TABLE 1 Definitions of anatomical and developmental traits influencing leaf trichome density (D_t).

Trait	Symbol	Unit	Definition
Trichome density	D_t	no. mm^{-2}	Number of trichomes per leaf area.
Stomatal density	D_s	no. mm^{-2}	Number of stomata per leaf area.
Epidermal pavement cell index	i_e	unitless	Number of pavement epidermal cells relative to total number of epidermal cell types [$n_e \div (n_s + n_t + n_e)$].
Stomatal index	i_s	unitless	Number of stomata relative to total number of epidermal cell types [$n_s \div (n_s + n_t + n_e)$].
Trichome index	i_t	unitless	Number of trichomes relative to total number of epidermal cell types [$n_t \div (n_s + n_t + n_e)$].
Epidermal area	e	mm^2	Projected area of epidermal pavement cell.
Stomatal area	s	mm^2	Projected area of epidermal stoma.
Trichome area	t	mm^2	Projected area area of epidermal trichome cell.
Stomatal number	n_s	no.	Total number of stomata.
Trichome number	n_t	no.	Total number of trichome cells.
Epidermal number	n_e	no.	Total number of epidermal pavement cells.

Hetherington and Woodward, 2003) has led to an enormous field of research into their development, structure and function (Buckley et al., 2003; Buckley, 2005; Franks and Beerling, 2009; Lin et al., 2015; Torii, 2021), and their potential association with trichomes. Given that a high D_t would contribute to maintained leaf function under high irradiance it might be co-selected with a high stomatal density (D_s), which would contribute to a high maximum rate of gas exchange and be especially advantageous for species adapted to shorter growing seasons by enabling rapid growth (Wong et al., 1979; Grubb, 1998; Hetherington and Woodward, 2003; Franks and Beerling, 2009; Lin et al., 2015). A number of studies across species have indicated a positive relationship between D_s and D_t (Skelton et al., 2012; Pan et al., 2021). However, detailed research in the species *Arabidopsis thaliana*, *A. halleri*, and *Nicotiana tabacum* has suggested an opposite relationship, i.e., a developmentally constrained trade-off between D_t and D_s due to their sharing precursor cells and both being reduced simultaneously by the greater cell spacing associated with larger epidermal cells (Glover et al., 1998; Yan et al., 2014; Adrian et al., 2015; Simon et al. 2020; Torii, 2021). Trichomes are initiated early in leaf development as protodermal precursors divide and then successively undergo cell fate determination, specification, and morphogenesis (Figure 1A; Larkin et al., 1997; Glover, 2000; Fambrini and Pugliesi, 2019; Torii, 2021). Protodermal cell divisions give rise to meristemoid mother cells (MMCs), which can either develop into trichomes themselves, or to stomatal meristemoid cells, which in turn divide into guard mother cells and finally guard cells (Figure 1A; Torii, 2021). In *Arabidopsis thaliana*, the molecular mechanisms within MMCs overlap between stomatal and trichome formation (Adrian et al., 2015). Thus, the high production of SPEECHLESS (SPCH) proteins in MMCs drives the initiation of the stomatal cell lineage

pathway (Torii, 2021) and upregulates the synthesis of TOO MANY MOUTHS (TMM), which drives a negative feedback loop that ensures one-cell-spacing between stomata and also reduces trichome numbers via an unknown mechanism (Yan et al., 2014). Yet, SPCH also upregulates the expression of the genes that drive trichome initiation, indicating a potentially direct role in trichome and stomatal development (Adrian et al., 2015; Torii, 2021). These molecular mechanisms may result in mutual inhibition between stomatal versus trichome formation during cell fate specification and development (Torii, 2021), resulting in a trade-off between D_s and D_t (Glover et al., 1998).

We aimed to clarify how and why a developmental trade-off may be overcome across diverse species. We disentangled the developmental origin of the relationship by deriving mathematical expressions for D_t and D_s as functions of anatomical variables of mature leaves that reflect their development, i.e, trichome and stomatal indices (i_t and i_s), and the area of epidermal pavement cells (e), trichome bases (t), and stomata (s) (Table 1). Our approach extends that of a previous study of stomatal variables as functions of developmental traits including stomatal index (i_s, the number of stomata per number of total epidermal cells), e and s (Sack and Buckley, 2016). In that study of glabrous-leafed species, species tended to achieve higher D_s through both higher i_s and lower e—that is, by initiating more stomata and by reducing spacing between them with smaller epidermal pavement cells (Sack and Buckley, 2016). The achievement of higher D_s through a higher i_s has been referred to as "active initiation" and that through smaller e as "passive dilution" for plants of given species grown under different light or vapor pressure deficits (Carins Murphy et al., 2012, 2014, 2016). Indeed, the ability to disentangle the effect of i_s on D_s from that of e, i.e., the effect of stomatal numbers independent of cell and leaf size, dates to Salisbury

(1927), and i_s has become a major trait used to quantify stomatal development and its influence on D_s independently of epidermal cell size, with application in studies of stomatal evolution and paleobiology (Royer, 2001; Konrad et al., 2021; Muir et al., 2022). In this study, we introduce the analogous variable i_t, which similarly resolves the contribution of increased trichome numbers to D_t, independently of cell and leaf size. We applied our equations for D_t and D_s to resolve these traits' developmental drivers, and the origin of their relationship across 78 angiosperm species of California ecosystems. We hypothesized that a positive D_s vs. D_t coordination would arise if developmental antagonism can be overcome by evolving greater numbers of precursor cells, which would enable development of both higher i_t and i_s, or through smaller e, which would reduce cell spacing and increase both D_t and D_s.

Further, we compiled studies of D_t–D_s relationships within and across species to determine the commonness of a trade-off vs positive coordination vs independence. Thus, a trade-off indicates coupling of high D_s with low D_t and high D_t with low D_s. Positive coordination indicates coupling of low D_t with low D_s and high D_t with high D_s. Independence would arise from decoupling of D_t and D_s.

Finally, we used heuristic modeling to examine how D_t–D_s relationships would influence the carbon balance and ecological filtering of a species pool colonizing habitats differing in light availability, water availability, and temperature and humidity, to establish the potential benefits of overcoming a developmental trade-off.

We thus derived the developmental basis for D_t, D_s, and their relationship across diverse species, tested the commonness of D_t–D_s relationship types, and analyzed how and why developmentally based trait relationships may arise across diverse species.

MATERIALS AND METHODS

Plant material

To quantify the basis of D_t and D_s across diverse species, we sampled 157 common angiosperm species at seven sites (19–41 species, depending on site) representative of ecosystems within the California Floristic Province (Appendix S1; alpine, chaparral, coastal sage scrub, desert, mixed conifer–broadleaf forest, mixed riparian woodland, and montane wet forest). From each of five individuals per species, we sampled fresh, fully expanded, mature leaves. For 78 of the 157 species, representative of 29 families, trichomes were apparent on leaf surfaces, and all epidermal cell types could be resolved and traits quantified using our methods (Appendix S1; Quantification of anatomical traits section below). Notably, many of the excluded 79 species also had trichomes but all epidermal cell type traits could not be quantified for this study. Additional details on field sampling and methodology can be found in a previous publication (Medeiros et al., 2023).

Sample anatomical preparation

Sampled leaves were fixed in formalin–acetic acid–alcohol (FAA; 37% aqueous formaldehyde, 13% glacial acetic acid, and 50% ethanol, v/v/v) solution. We quantified epidermal traits from micrographs taken from nail varnish impressions of the abaxial and adaxial leaf surfaces (Medeiros et al., 2019) for one leaf for each of the five individuals per species, imaged with a light microscope (40× objective; Leica Lietz DMRB; Leica Microsystems, Wetzlar, Germany) and a camera with imaging software (SPOT Imaging Solution, Diagnostic Instruments, Sterling Heights, MI, USA).

Quantification of anatomical traits

From the leaf micrographs, we measured the areas of individual trichome bases (t), stomata (s; one guard cell pair) and epidermal pavement cells (e), and trichome, stomatal and epidermal densities (D_t, D_s and D_e; number of cells or stomata per mm^2) for both abaxial and adaxial surfaces (Medeiros et al., 2019). For each image, we distinguished quadrants by drawing central vertical and horizontal lines, and measured the area of four stomata, two epidermal pavement cells, and one to four trichome bases from distinct quadrants as centrally as possible, given visibility. Traits were quantified using the software ImageJ (Rasband, 1997–2018). We traced stomatal and pavement cell outlines to measure s and e and estimated t by measuring the semi-major and semi-minor axes (a and b, respectively) of the trichome cell base and calculating the area of an ellipse as area = πab. Trichome and stomatal cell densities (D_t and D_s) were calculated by counting the number of trichomes and stomata and dividing these values by the area of the image. For epidermal cell density (D_e), we counted the number of epidermal cells for two of the four quadrants, divided these numbers by the areas of the respective quadrants, and then averaged these two values. D_e was assessed for images for three to five individuals per species, i.e., when the image quality assured accurate cell counts. As our measures of cell densities were sometimes from different individuals per species, we calculated mean trichome and stomatal indices (i_t and i_s) at the species level using species mean values for the numbers of trichomes and stomata, respectively, per total number of trichomes, stomata, and epidermal pavement cells (Salisbury, 1927; Sack and Buckley, 2016).

Our method for measurement of epidermal traits was successful for most leaves, for trichome densities up to 360 mm^{-2}, though not for very densely hairy leaves, for which D_t and other epidermal traits cannot be resolved from impressions. We acknowledge and emphasize the need for further studies of D_t for the hairiest leaves; scanning electron microscopy of shaved leaves (Hoof et al., 2008) can work in some cases, but not others. Further, for some leaves, epidermal irregularities prevented assessment of epidermal pavement cell numbers or sizes. For 78 species,

measurements could be made of all traits for one or both leaf surfaces; for 37 of the 78 species, both surfaces could be measured, but for 26 species, only on the adaxial surface, and for 15 species only on the abaxial surface (Appendix S1). For species in which measurements could only be made for one surface and not the other, this difficulty was typically due to inability to assure accuracy in epidermal pavement cell number or trichome base diameters. Thus, for analyzing the developmental basis of trichome density, we present data for all 78 species, but for species for which all variables were quantifiable for only one surface, we present data only for that surface (Appendix S1). Almost all of the 78 species were amphitrichomous and 2/3 of these were amphistomatous (Appendix S1). For 24 amphistomatous and for 13 hypostomatous species, we had complete data for both surfaces. For 46 of the 78 species, we could also determine from our micrograph images the trichome types present, i.e., simple, pilate/capitate, peltate or stellate, and glandular or nonglandular (Appendix S1). Trichomes of the simple type are single-stalked, without a distinct secretory cell tip, and either unicellular or multicellular uniseriate (Werker, 2000). Pilate and capitate trichomes are single stalked, with a secretory cell tip; pilate trichomes have elongated stalks, though the stalks were not discernible in our images (Werker, 2000). Peltate trichomes are also single stalked, with multicellular secretory cells at the head of the stalk (Werker, 2000). Stellate trichomes are star-shaped with several elongated arms attached to a common base (Werker, 2000). Lastly, glandular trichomes possess a secretory cell at the tip of the trichome, capable of secreting specialized metabolites (Werker, 2000).

Derivation of leaf trichome density and stomatal density on the basis of developmental traits

We derived a novel equation for leaf trichome density (D_t) on the basis of developmental traits i_t and i_s and anatomical traits t, s, and e to enable calculation of how quantitative changes in size and initiation of epidermal cell types influence D_t. We derived a similar equation for the D_s of trichomous species, given that the original study that derived D_s as a function of developmental variables focused on glabrous-leafed species and thus did not include i_t or t (Sack and Buckley, 2016).

Meta-analysis of the relationship between leaf trichome and stomatal densities

We compiled studies that included analyses of the relations between leaf trichome density and stomatal density for individuals, genotypes, or populations of a species, or for distinct species, from published literature via searches using Google Scholar, Web of Science, and references from articles (Table 2). We searched for studies using the keywords "leaf trichome density" and "leaf stomatal density" combined with "coordination", "association", "relationship", and "development".

Statistical and comparative analyses

For the six species that were sampled in two sites (Appendix S1), we averaged traits across individuals within each site, then averaged the two species values for each site.

Analyses were performed using the R version 4.2.3 (R Core Team, 2023). To validate the correctness of our mathematical derivation of the developmental basis of leaf trichome density, we tested relationships of measured D_t with that estimated from Eq. 6 (given in Results) for the abaxial and adaxial surfaces using ordinary least squares (OLS) regressions with a fixed zero intercept using the SMATR package (Warton et al., 2012). Similarly, we implemented the same analysis to validate the correctness of our mathematical derivation of leaf stomatal density (D_s). Validation of the mathematical derivations were indicated by a high R^2 and by the 1:1 line falling within the 95% prediction intervals of the tested relationships (Sack and Buckley, 2016).

We tested for potential trade-offs or positive coordination in trichome and stomatal densities (D_t and D_s) and in trichome and stomatal initiation rates (i_t and i_s) using standard major axes (SMA) (Warton et al., 2012). For the 78 species, we tested these relationships across the adaxial and abaxial surfaces for the 39 and 52 species, respectively, for which we had complete data (Appendix S1).

We tested the quantitative impact of the variables that determine leaf D_t using two sensitivity analyses. First, we tested the "intrinsic sensitivity" of D_t to each input variable from Eq. 6 (given in Results), i.e., how D_t varied when each variable was changed from zero to 200% of its mean across species, maintaining all other variables constant at their mean value (John et al., 2017). Thus, 100% would indicate mean values of the driver variables, and 200% would indicate increasing this mean by 100%. Second, we tested the "realized sensitivity" of D_t and D_s to each input variable by partitioning the realized contribution of each input variable to the differences in D_t or D_s for each pairwise species combination, and then calculating the median contribution across all pairwise species combinations (Buckley and Diaz-Espejo, 2015; John et al., 2017). A higher positive percentage contribution indicates that the variable plays a stronger realized role in determining D_t or D_s across the species set. By contrast, a variable with a negative percentage for the realized contribution indicates that for a species with higher D_t or D_s, that variable differed across species in the direction that would have caused a lower D_t or D_s, and this negative effect is overcome by positive effects of the other variables. Because the total causal contributions often departed slightly from 100% due to "averaging error", i.e., Jensen's inequality, by which the average of outputs of a nonlinear function differs from the function applied to average input variables (Denny, 2017), we rescaled the partitioning outputs as

TABLE 2 Published studies showing variation in the association of leaf trichome and stomatal densities within and across species. For each study, we report whether or not the study supported evidence of a trade-off (TO; i.e., decreasing trend), positive coordination (PC; i.e., increasing trend) or independence (I; i.e., no trend) in trichome and stomatal densities, sampled species and family, scale at which the comparison was made, growing conditions, leaf surface tested (Ab, abaxial; Ad, adaxial), and the reference. References ordered by their support for a trade-off, positive coordination, or independence. For the leaf surface, NA indicates information about the leaf surface tested was not provided in the study.

Relationship of trichome density vs. stomatal density	Species	Family	Scale	Growing conditions	Leaf surface	Reference
TO	Arabidopsis halleri	Brassicaceae	Between 2 populations	Field sites	Ad	Simon et al. (2020)
TO	Nicotiana tabacum	Solanaceae	Between wild and transgenic individuals	Not reported	Ad; Ab	Glover et al. (1998)
PC	Artemisia tridentata	Asteraceae	Between 2 populations	Common garden	NA	Downs and Black (1999)
PC	Cymbopogon citratus	Poaceae	Between individuals within water-deficit treatments	Experimental water-deficit and arbuscular mycorrhizal fungi	NA	Mirzaie et al. (2020)
PC	Dendrobium bellatulum, D. carinferum, D. draconis, D. longicornu, D. trigonopus, D. williamsonii	Orchidaceae	Across 6 species	Common garden	Ab	Pan et al. (2021)
PC	Leucadendron spp., Leucospermum spp., Protea spp.	Proteaceae	Across 18 species and within Leucadendron conocarpodendron	Common garden	Ad	Skelton et al. (2012)
PC	Quercus faginea, Q. suber and Q. ilex	Fagaceae	Within each species	Field sites	Ab	Mediavilla et al. (2019)
PC	Quercus variabilis	Fagaceae	Across 44 natural and 15 common garden populations	Natural and common gardens	NA	Zhu et al., 2023 [preprint]
PC	Solanum pennellii	Solanaceae	For 2 genotypes between well watered and water-deficit experiments	Experimental water-deficit	Ad; Ab	Zsögön (2011)
I	Capsicum annuum	Solanaceae	Across 7 varieties	Common garden	Ad; Ab	Serrano-Mejía et al. (2022)
I	Solanum lycopersicum	Solanaceae	Between 4 varieties	Well-watered and experimental water-deficit	Ad	Galdon-Armero et al. (2018)
I (Ad, 1 variety); TO (Ad, 1 variety); PC (Ab, both varieties)	Trichosanthes cucumerina L.	Cucurbitaceae	Across experimental salt-stress treatments for 2 varieties	Experimental salt-stress	Ad; Ab	Adebooye et al. (2012)
I (Ad, both varieties); PC (Ab, both varieties)	Digitaria insularis	Poaceae	Between 3 vegetative stages and for 2 varieties	Experimental glyphosate	Ad; Ab	Barroso et al. (2015)
I (Ad); PC (Ab)	Lens spp.	Fabaceae	Across 12 varieties	Growth chamber	Ad; Ab	Patel et al. (2021)

TABLE 2 (Continued)

Relationship of trichome density vs. stomatal density	Species	Family	Scale	Growing conditions	Leaf surface	Reference
I (Ad); PC (Ab)	Solanum melongena	Solanaceae	Between experimental water-deficit treatments	Experimental water-deficit	Ad; Ab	Fu et al. (2013)
TO; PC; I (population specific)	Quercus brantii	Fagaceae	Within populations	Field sites	NA	Soheili et al. (2023)
PC; PC; TO; PC (species specific); I (across species)	Tillandsia balbisiana, T. juncea, T. streptophylla and T. utriculata; Aechmea bracteata, Catopsis nutans, T. balbisiana, T. brachycaulos, T. dasyliriifolia, T. elongata, T. fasciculata, T. juncea, T. recurvata, T. schiedeana, T. streptophylla, T. usneoides, T. utriculata, T. yucatana	Bromeliaceae	Within individuals of each of four species; across 14 species of Bromeliaceae	Field sites	Ab	Cach-Pérez et al. (2016)

percentages of the total, so all numbers add up to 100%. Notably, the realized contributions of the underlying variables in a realized sensitivity analysis depends on the variation of all variables and thus on the species set (John et al., 2017). To enable robust comparisons of the realized sensitivity of D_t and D_s to input variables on both leaf surfaces, this analysis focused on the 37 species for which data were available for D_t and D_s for both surfaces, separately considering the 24 amphistomatous species, i.e., with $D_s > 0$ on both surfaces, and the 13 hypostomatous species, i.e., with D_s of 0 on the adaxial surface.

Overall, the "intrinsic sensitivity" analysis provides a theoretical understanding of the quantitative consequences for shifts in the variables of an equation, and the "realized sensitivity" is similar but represents the impact of shifts in multiple variables of an equation, which is more likely to occur in nature.

Modeling the carbon balance impacts of multifunctionality of leaf trichome density in association with stomatal density

To assess the carbon balance consequences of a range of potential developmental associations between trichome and stomatal density, we simulated leaf gas exchange and energy balance for a range of environmental conditions, and for each of three imaginary "species sets" in which D_t and D_s were positively or negatively associated or uncorrelated (reflecting hypothetical developmental constraints or a lack thereof). We defined "carbon balance" narrowly as net photosynthesis minus two amortized costs: one proportional to transpiration rate, representing the carbon cost of acquiring water and transporting it to leaves, and another proportional to trichome density, representing the carbon cost of building leaf hairs. In most respects, this gas exchange model was based on established biophysical relationships, including the photosynthesis model of Farquhar et al. (1980) and an energy balance for estimating leaf temperature; details of those features of the model are described in Appendix S2. We extended standard modeling practice in three ways: (1) attempting to account explicitly for the effects of trichomes on light capture and boundary layer resistance, (2) assuming stomatal conductance is proportional to stomatal density, and (3) repeating calculations for three simulated sets of species that differed in the joint distributions of trichome and stomatal densities. For (1), we assumed that both albedo (leaf reflectance to visible light, ρ) and boundary layer resistance to water vapor (r_{bw}) increase with trichome density:

$$\rho = \rho_{min} + (\rho_{max} - \rho_{min}) \cdot \frac{H}{H + 1} \quad (1)$$

$$r_{bw,x} = r_{bwmin} + (r_{bwmax} - r_{bwmin}) \cdot \frac{H_x}{H_x + 1}, \quad (2)$$

where H is relative trichome density (actual trichome density divided by the population median); ρ_{min} and ρ_{max} are the values of albedo with no trichomes present, and in the limit of infinite trichome density, respectively; r_{bwmin} and r_{bwmax} are likewise values of r_{bw} with no or infinite trichomes, respectively; and $r_{bw,x}$ and H_x are boundary layer resistance and H calculated for a single surface, where x denotes either abaxial or adaxial. Thus, ρ and r_{bw} each increase with trichome density in saturating fashion. For (2), we assumed a fixed proportionality between stomatal conductance to water vapor (g_{sw}) and stomatal density (D_s) such that g_{sw} (in mol m^{-2} s^{-1}) = 0.001(D_s/mm^{-2}); thus, for example, a leaf with $D_s = 200$ mm^{-2} would have $g_{sw} = 0.2$ mol m^{-2} s^{-1}. For (3), we applied the model to each member of three "species sets" simulated using the observed marginal density distributions for the California species for each variable (abaxial and adaxial D_s and D_t) but resampled to represent three scenarios: whole-leaf D_s and D_t are completely uncorrelated ("independent" set), perfectly negatively correlated due to a developmental trade-off ("trade-off"), or perfectly positively correlated due to a positive developmental constraint ("positive coordination"). We applied these calculations under a range of environmental conditions to identify conditions favoring each imaginary species set, and present results for three environments defined by moisture, temperature, humidity, and windspeed: (1) high moisture and humidity, mild temperature, and low wind (amortized water cost [χ_w] = 400 μmol CO_2 mol^{-1} H_2O, air temperature [T_{air}] = 25°C, water vapor [w_{air}] = 0.02 mol mol^{-1}, and windspeed [v_w] = 1 m s^{-1}); (2) low moisture, dry air, high temperature, and low wind ($\chi_w = 1000$ μmol CO_2 mol^{-1} H_2O, $T_{air} = 45$°C, $w_{air} = 0.01$ mol mol^{-1}, and $v_w = 1$ m s^{-1}); and (3) intermediate moisture, humidity and temperature, and high wind ($\chi_w = 700$ μmol CO_2 mol^{-1} H_2O, $T_{air} = 35$°C, $w_{air} = 0.015$ mol mol^{-1}, and $v_w = 5$ m s^{-1}). The water cost, χ_w, which is used to turn transpiration into a cost that can be subtracted from photosynthesis, represents the carbon costs of acquiring water from the soil and transporting it to leaves; χ_w would be large in environments with scarce water because more carbon would need to be invested in roots and xylem to take up and transport a given amount of water. Procedures used to create and simulate these populations are described in more detail in Appendix S2.

RESULTS

Derivation and validation of an expression of the basis for D_t in developmental traits

We derived equations for trichome density (D_t, no. trichomes mm^{-2} leaf area) and stomatal density (D_t, no. stomata mm^{-2} leaf area) as functions of underlying epidermal anatomical traits with proximal relationship to development, i.e., trichome and stomatal indices (i_t and i_s, respectively), and the areas of trichome cell bases (t), stomata (s), and epidermal

pavement cells (e) (Table 1). The i_t is analogous to the i_s introduced by Salisbury (Salisbury, 1927) as a means to correct D_t for the effect of larger epidermal cells in spacing stomata apart; these indices correspond to the number of trichomes (n_t) or stomata (n_s) divided by the sum of n_t, n_s, and the number of epidermal pavement cells (n_e). Thus, the i_t and i_s are related to n_t, n_s, n_e, t, s, and e as:

$$i_t = \frac{n_t}{n_t + n_s + n_e}, \quad i_s = \frac{n_s}{n_s + n_t + n_e}. \quad (3)$$

D_t is related to n_t, n_s, n_e, t, s and e as:

$$D_t = \frac{n_t}{\text{Total area}} = \frac{n_t}{n_t t + n_s s + n_e e}$$
$$= \frac{1}{t + \frac{n_s}{n_t}s + \frac{n_e}{n_s}\frac{n_s}{n_t}e}, \quad (4)$$

where Total area is that of the entire leaf surface with trichomes and/or stomata (mm^2). Noting that $n_e/n_s = i_e/i_s$, and $n_s/n_t = i_s/i_t$, Eq. 4 can be rearranged as:

$$D_t = \frac{1}{t + \frac{i_s}{i_t}s + \frac{i_e}{i_s}\frac{i_s}{i_t}e}. \quad (5)$$

Applying $i_e = 1 - (i_s + i_t)$ to Eq. 5 gives:

$$D_t = \frac{i_t}{i_t t + i_s s + (1 - i_t - i_s)e}. \quad (6)$$

An equation for D_s for trichomous species can be derived by swapping i_s for i_t, and s for t in Eq. 6:

$$D_s = \frac{i_s}{i_s s + i_t t + (1 - i_s - i_t)e}. \quad (7)$$

We validated Eqs. 6 and 7 using data for the 78 diverse angiosperm California species, for which D_t varied from 4.51 trichomes mm^{-2} for *Adenostoma fasciculatum* to 310 trichomes mm^{-2} for *Antennaria media* on the abaxial surface, and from 5.09 trichomes mm^{-2} for *Cercocarpus betuloides* to 418 trichomes mm^{-2} for *Eriogonum douglasii* on the adaxial surface (Figure 2A, B; Appendix S1). For both D_t and D_s, the observed and estimated values from Eqs. 6 and 7 were closely related, and lines fitted through the origin across abaxial and adaxial surfaces had 95% prediction intervals that included the 1:1 line (Figure 2A, B; Appendix S1; $R^2 = 0.98$–0.99, slope $b = 0.91$–0.94).

Instrinsic sensitivity of D_t and D_s to its developmental drivers

Equations 6 and 7 enable analyses of the developmental determinants of differences in D_t and D_s. In an intrinsic sensitivity analysis, which shifts each anatomical driver of

D_t and D_s in trichomous leaves from their mean values while holding other anatomical drivers constant at their mean values, i_t and e most strongly influence D_t, whereas i_s and e most strongly influence D_s. Our finding for the role of traits in determining D_s is congruous with that shown for non-trichomous leaves previously (Sack and Buckley, 2016). Notably, while i_t positively influences D_t and i_s positively influences D_s, e has a negative influence on both, because larger e spaces specialized cell types farther apart (Figure 3A, B; Appendices S3–S6). The other variables have much lower intrinsic impacts on D_t. The influence of i_s is positive for D_t, because differentiating more epidermal cells with generally small stomata would result in trichomes spaced more closely, and similarly, the influence of i_t is also positive for D_s. The intrinsic influences of t and s are negative on both D_t and D_s, because larger cells space

trichomes and stomata farther apart (Figure 3A, B; Appendices S3–S6).

Realized sensitivity of D_t and D_s with respect to developmental traits in California angiosperm species

The 78 California species included diverse trichome types, i.e., simple, pilate/capitate, peltate and stellate, and glandular and nonglandular (Appendix S1). Across these diverse species, the variation in D_t and D_s would be driven by simultaneous changes in multiple anatomical variables as shown by Eqs. 6 and 7. For example, a higher D_t may arise if a species has higher i_t or lower e, and especially if it has both. Thus, we examined the realized sensitivity of D_t and
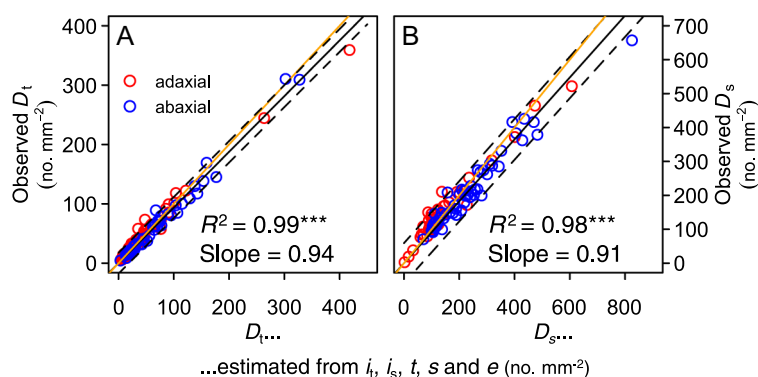

FIGURE 2 Validating the developmental basis for leaf trichome density and analyzing the contributions of anatomical and developmental traits to leaf trichome density for diverse California species. Estimation of adaxial and abaxial (A) leaf trichome density (D_t), and (B) leaf stomatal density (D_s) as functions of the trichome index (i_t), stomatal index (i_s), trichome cell area (t), stomatal cell area (s) and epidermal pavement cell area (e), plotted against measured values of D_t and D_s. ***$P < 0.001$. Black solid lines in both panels are ordinary least square regressions (OLS) fitted to the data with a fixed zero intercept, with the 1:1 line in orange and 95% prediction intervals as segmented black lines. $N = 63$ and 54 in (A) and $N = 39$ and 51 in (B), corresponding to adaxial and abaxial surfaces, in red and blue, respectively. The total species number represented by both surfaces for both traits was 78.
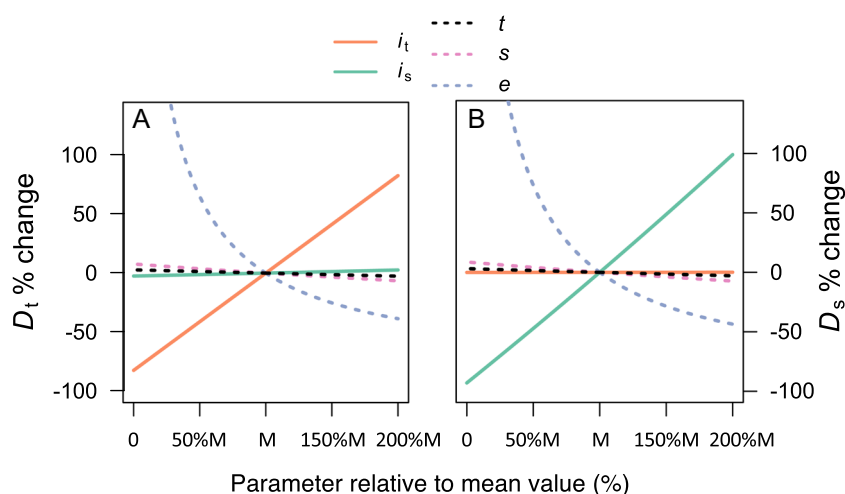

FIGURE 3 Intrinsic sensitivity of leaf trichome and stomatal densities to underlying developmental parameters. Intrinsic sensitivity of (A) D_t and (B) D_s, for the abaxial surface (Appendices S3 and S4). The intrinsic sensitivity for the adaxial surface was similar to that of the abaxial surface (Appendices S5 and S6). The intrinsic sensitivity signifies the impact on D_t or D_s of shifting one variable in Eqs. 6 and 7, while holding all others constant.

D_s, i.e., the importance of its determinant traits in driving their variation for a subset of 24 amphi- and 13 hypostomatous California angiosperm species for which we had data for all input variables (Figure 4). We found the determination of D_t was similar for both surfaces, and for amphi- and hypostomatous leaves, whereas that of D_s differed depending on the surface and stomatal distribution (Appendix S7). On average for the two surfaces of amphistomatous species and the abaxial surface of hypostomatous species, i_t accounted for the bulk (76–90%) of variation in D_t across species and e for a substantial minority of variation (8.0–21%), and i_s, s and t contributed negligibly on average. For D_s, for amphistomatous species, i_s accounted for the majority of variation (68%) on the adaxial surface and e for a substantial minority of variation (30%), whereas on the abaxial surface, e accounted for the majority (57%) of variation in D_s across species and i_s a minority (37%); in all cases, on average, t and s contributed negligibly to variation in D_s across species (Figure 4; Appendix S7). Similar determinants of D_s, i.e., i_s and e, were observed for the abaxial surface of hypostomatous species. Yet, variation in s accounted for 6% of across species variation in D_s for the abaxial surface of hypostomatous species (Appendix S7).

Positive coordination of D_t and D_s and its developmental basis in California angiosperm species

Across the data set for California angiosperm species, D_t and D_s were positively related on the adaxial and abaxial surfaces (Figure 5A; $N = 39$ and 52, respectively;

$r = 0.51$–0.62, $P < 0.001$). In both cases, this positive coordination was driven both by the association between i_t and i_s across species, which were major drivers of, respectively, D_t and D_s (Figure 5B; $r = 0.33$–0.4, $P < 0.05$), and by the influence of small e as a minor driver of high D_t and substantial driver of high D_s across species (Figure 4A, B).

Meta-analysis of published relationships of D_t and D_s within and across diverse species

Our meta-analysis was based on a compilation of 17 studies with leaf trichome and stomatal densities across diverse species, or across populations or genotypes of given species, or for plants of given species grown under different experimental treatments (Table 2). Among 17 studies, 13 (76%) supported positive D_t–D_s coordination, 5 (29%) a trade-off, and 7 (47%) independence (Table 2). Notably, 6 of the 17 (35%) studies showed mixed results, depending on specific comparison sets (i.e., abaxial vs adaxial, or comparisons between populations or genotypes within species of given studies). Trade-offs and independence in D_t and D_s were found particularly in studies focusing within species, including *Arabidopsis helleri*, *Artemisia tridentata*, *Capsicum annuum*, *Digitaria insularis*, *Nicotiana tabacum*, *Quercus brantii*, *Solanum lycopersicum*, *Solanum melongena*, *Tillandsia streptophylla*, and *Trichosanthes cucumerina* (Table 2). By contrast, the positive coordination of D_t and D_s is much more general and found across many taxonomic scales, including across species of different plant families (Figure 5), across species within a family (e.g., Proteaceae), across species within a genus (e.g.,
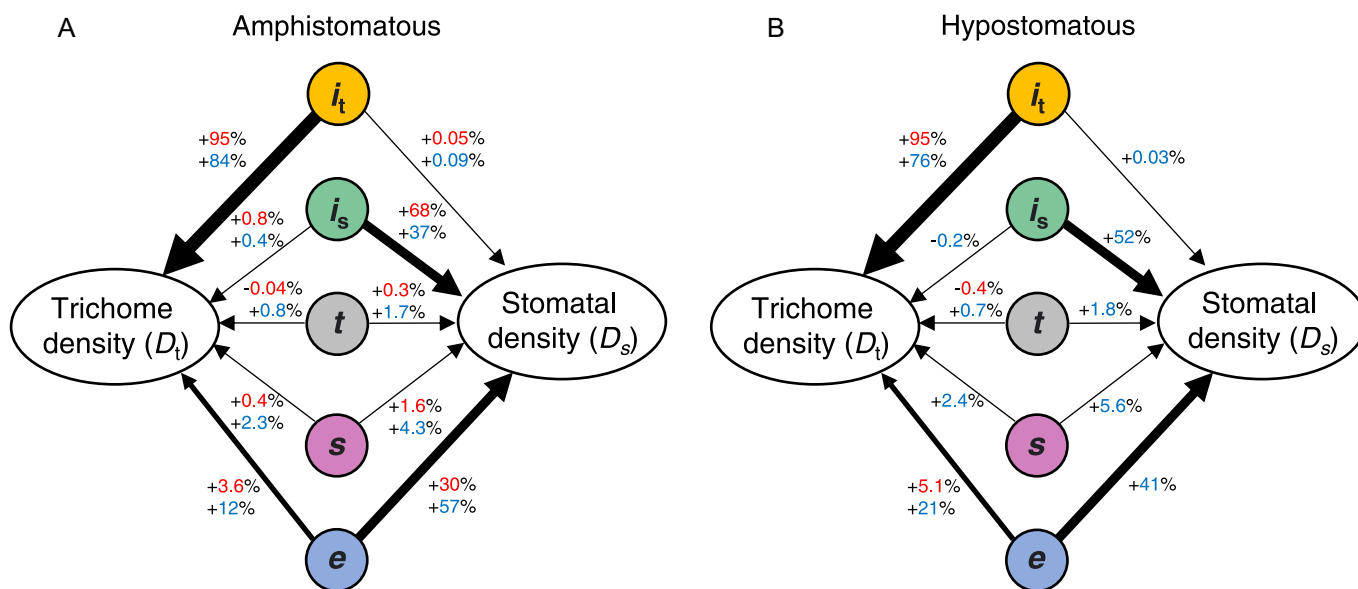

FIGURE 4 Contributions of anatomical and developmental traits to leaf trichome density for diverse California species. The realized sensitivity of D_t and D_s to underlying developmental variables for (A) amphistomatous and (B) hypostomatous leaves. Realized influences are presented as percentages adjacent to arrows, with the upper red value for the adaxial surface and lower blue value for the abaxial surface; the thickness of the arrows reflect relative realized influences (Appendix S7).
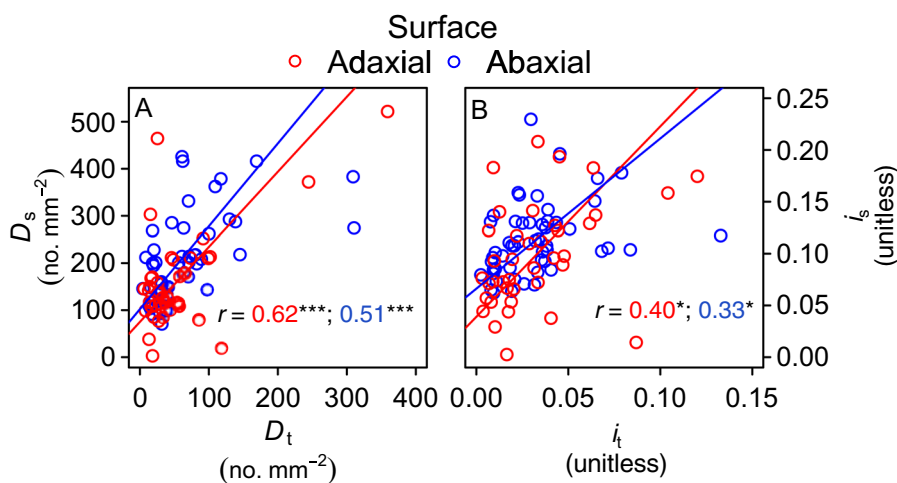
FIGURE 5 Testing the association of leaf trichome density (D_t) with stomatal density (D_s), and trichome initiation rates (i_t) with stomatal initiation rates (i_s) across diverse California species. Relationships of (A) trichome density (D_t) with stomatal density (D_s) and (B) leaf trichome index (i_t) and stomatal index (i_s), for the adaxial and abaxial leaf surfaces, in red and blue points, respectively. $N = 39$ and 52 in both panels, corresponding to adaxial and abaxial surfaces, in red and blue, respectively. Lines are standard major axes (SMA) regressions. $*p < 0.05$, $***p < 0.001$.

Dendrobium), between isolated populations for several species, between genotypes of several crop species, and between individuals grown under experimental treaments such as salt or water stress, and for both adaxial and abaxial leaf surfaces (Table 2).

Impacts of the association of trichome and stomatal densities on the carbon balance of species sets

We conducted a theoretical heuristic analysis using a biophysical model of leaf gas exchange and energy balance to simulate the impacts on carbon balance of variation in D_t and D_s according to several scenarios. We simulated species sets by resampling from the marginal distributions of D_t and D_s in the California species to produce species sets with D_t and D_s positively or negatively associated or independent (Figure 6). For each species, we modeled carbon balance based on its D_t and D_s. For each species set, we identified a hypothetical set of environmental conditions favoring that species set above the others.

In a wet and mild environment, species with high D_s achieve high photosynthetic rates, and light reflectance by trichomes has little benefit because abundant water allows leaves to use all the available light. Thus, the D_t–D_s trade-off scenario gives greater carbon balance than the positive D_t–D_s association scenario (Figure 6). However, a strict D_t–D_s trade-off constrains the highest D_s values, and the independent scenario has greater potential carbon balance (Figure 6). Under dry and hot conditions, high D_s has little advantage because scarce water would limit stomatal opening, whereas trichomes are beneficial because they cool the leaf by reflecting excess light (which cannot be used in photosynthesis due to low stomatal conductance).

Notably, high D_t can have especially beneficial impacts when D_s is low because trichomes additionally would increase boundary layer resistance, which decouples leaf and air temperature, and thereby enables the leaf to more effectively cool below air temperatures via transpiration. Thus, the D_t–D_s trade-off scenario has the highest carbon balance in the hot and dry environment (Figure 6). In an environment with intermediate moisture but high wind, the benefits of trichomes for increasing the boundary layer are reduced, and the loss of this benefit would favor low D_t especially at low D_s (where photosynthetic rate is lower, because trichomes reduce photosynthesis due to light reflection) overall favoring the positive coordination scenario (Figure 6).

We note that these theoretical simulations should not be interpreted literally, given the inclusion of only some potential trichome functions and not others, and arbitrary parameterization with all else being equal across species varying in D_t and D_s. Yet, this heuristic cost–benefit analysis demonstrated that the most beneficial coordination (or independence) of trichome and stomatal densities would differ strongly across environments.

DISCUSSION

We found that, despite the developmental conflict between D_t and D_s identified in the species *Arabidopsis thaliana, A. halleri*, and *Nicotiana tabacum* (Glover et al., 1998; Yan et al., 2014; Simon et al., 2020), a trade-off can be circumvented across diverse species. Our derivation of a novel equation for leaf trichome density (D_t) and D_s on the basis of developmental traits i_t and i_s, e, s, and t enables calculation of how quantitative shifts in size and initiation of epidermal cell types influence D_t and D_s. These equations
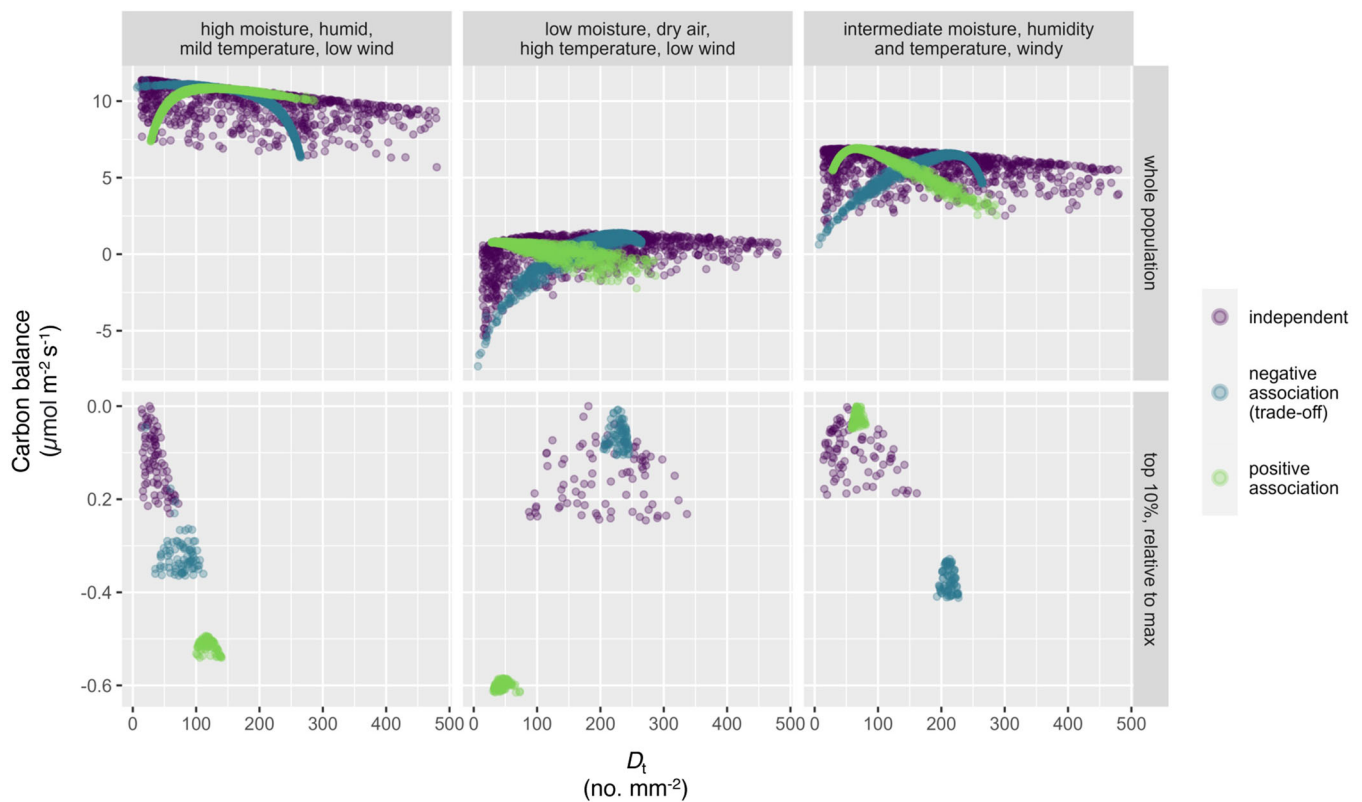
FIGURE 6 Heuristic predictions of carbon balance (leaf photosynthesis net of leaf respiration and the amortized carbon costs of leaf hair construction and of water uptake and transport). Theoretical simulations were tested for three hypothetical environments, and three sets of species based on the marginal distributions of diverse California species for stomatal and trichome densities (D_s and D_t, respectively), resampled to produce three $D_s.D_t$ associations, i.e., "independent", or a perfect negative correlation representing a developmental ("negative association" [trade-off]), or a perfect positive correlation representing developmental coordination ("positive association"). The upper panels show results for all species in each species set, across the full range of D_t; the lower panels show the top 10% of each species set by carbon balance, illustrating that different developmental constraints, or lack thereof, would maximize carbon balance in different environments.

enabled deeper realized analysis for California species of the drivers of D_t and D_s and their coordination and showed that i_t and i_s were positively rather than negatively related, and this positive coordination, in addition to the common influence of e on both D_t and D_s, propagated to a coordination of D_t and D_s. Further, in the meta-analysis of previous studies, a positive coordination of D_t and D_s was the most general pattern (Table 2). Finally, our theoretical model simulations showed that the most adaptive association of D_t and D_s with respect to carbon balance would depend on the environment, with a trade-off being optimal only under certain conditions, and a positive coordination or decoupling of D_t and D_s in others.

Our sensitivity analysis of the developmental drivers of D_t and D_s according to Equations 6 and 7 showed their determination by shared and different factors. All else being equal, a high D_t is principally achieved by increasing i_t, due to the initiation of a higher proportion of trichomes from epidermal precursors, with an additional lesser role of small epidermal pavement cell size (e) decreasing the spacing between trichomes (Figure 3A, B), similarly to the roles of i_s and e in determining D_s previously described for stomata in glabrous-leafed species (Salisbury, 1927; Sack and

Buckley, 2016). Yet, our realized analysis, which clarifies the true drivers of variation in D_t and D_s against the background of variation in all input variables, indicated slightly contrasting developmental drivers of D_t and D_s: a higher D_t was driven strongly by i_t and marginally by e, whereas for D_s the drivers differed for the two leaf surfaces, with adaxial D_s being more strongly driven by i_s, followed by e, and abaxial D_s more strongly driven by e, followed by i_s. This variation between leaf surfaces in cell differentiation was consistent with previous studies showing independent molecular controls on development and anatomy of adaxial and abaxial leaf surfaces (Figure 4; Kidner and Timmermans, 2010; Yamaguchi et al., 2012). Thus, because both D_t and D_s are impacted by changes in i_t and i_s, respectively, and e, the difference in the impacts of i versus e on D_t and D_s may arise from differences in the temporal aspects of trichome versus stomatal development and maturation. Although trichome cell fate determination occurs early during development in *A. thaliana*, our finding that D_t was more strongly determined by i_t and less by e, whereas D_s was less strongly determined by i_s and more by e, may indicate that for other plant species, trichome initiation might continue for longer than stomatal initiation,

and even as epidermal cells are still expanding. Additionally, shedding of trichomes between early development and leaf maturation (Choinski and Wise, 1999; Fernández et al., 2014) may also contribute to the lesser impact of e on D_t because the shedding of trichomes would be represented in i_t and would thus shift D_t independently of changes in e. Indeed, that D_t varies between immature and mature leaves indicates that the critical functions of D_t likely differ for immature and mature leaves. The lesser impact of e on D_t may also arise from packing density limitations due to differences in trichome morphologies with differing sizes, e.g. simple vs. stellate (Figure 1; Appendix S1). We note that the effect of larger e in reducing D_t and D_s (referred to as a "passive dilution" effect; Brodribb et al., 2013; Carins Murphy et al., 2016) could also be coupled with changes in vein density (Brodribb et al. 2013).

The positive relationship of D_t and D_s across a set of diverse California angiosperm species, similar to that reported in other studies within and across species (Table 2), is consistent with coordinated trait evolution and/or plasticity in response to the environment. For the California angiosperm species in our study, this positive relationship arose from the coordination of i_t and i_s, and from the contribution of small e to high D_t and D_s. Notably, some previous studies within species, especially of genetic TMM mutants and overexpressed TMM lines in *A. thaliana*, indicated negative relations between D_t with D_s, attributed to an allocation trade-off of epidermal precursor cells, driven by mutual inhibition in the development of trichomes vs stomata (Yan et al., 2014; Simon et al., 2020). Our finding of a positive relationship between i_t and i_s across a set of diverse species indicates that during diversification any allocation trade-off between trichome and stomata precursors was superseded by a positive coordination between trichome and stomatal initiation rates. In theory, such positive coordination could arise from increasing total precursor number or from loss of mutual inhibition of trichomes vs stomata (Adrian et al., 2015).

In the meta-analysis, we found much more support for positive D_t–D_s coordination and decoupling than for their trade-off. This variation in D_t–D_s relationships across studies indicates a lack of strict developmental constraint on this relationship and, thus, the possibility that species can adapt to a wide range of combinations and that different sets of genotypes or species can vary in the D_t–D_s association depending on adaptive context. Thus, trade-offs in D_t and D_s may arise in adaptation of species or genotypes to environments wherein a high D_t coupled with low D_s, or low D_t coupled with high D_s would provide advantages depending on the numerous functions of trichomes.

Multiple explanations may underlie this coordination across diverse species. First, under higher irradiance, where greater D_s would promote higher maximum rates of gas exchange, a higher D_t may be beneficial to reflect excess irradiance, maintain lower leaf temperatures, and improve water-use efficiency (Camargo and Marenco, 2011). Second,

a high D_s to achieve higher maximum gas exchange rates can contribute to "drought avoidance", i.e., rapid growth in shorter growing periods when water is available (Grubb, 1998; Hetherington and Woodward, 2003; Sack and Buckley, 2016). When trichomes benefit water relations, through improved foliar surface water uptake or enabling more rapid shedding of rain and thus resumption of photosynthesis due to repellency (Brewer et al., 1991), positive coordination in D_t and D_s would be advantageous by allowing for maintained gas exchange. Third, faster growing plants may have higher D_s and may especially benefit from hairs as a specialized defense to resist insect damage, given their generally higher leaf nutrient concentrations (Grubb, 1992, 1998). Finally, because plants with high D_s have greater likelihood of disease susceptibility due to pathogens entering through stomata (Gudesblat et al., 2009), a high D_t may entrap spores and prevent their contact with the epidermis (Gupt et al., 2021); thus, a high D_t would reduce the cost of a high D_s. Indeed, the advantages of such coordination would be especially important for more vulnerable, young, developing leaves when the numerous functions of trichomes are even more important (Karabourniotis and Fasseas, 1996; Choinski and Wise, 1999) and given the higher cost of developing a leaf with high D_s (Franks and Beerling, 2009). Despite the evidence for positive coordination between trichome and stomatal densities in our novel California angiosperm data set and in the previously published data sets, it is evident that some species can have high D_s but low D_t (Figure 5A, Table 2), and thus positive coordination may reflect a "missing quadrant" rather than a strict association.

Indeed, our heuristic modeling showed that the pattern of D_t–D_s developmental coordination that maximizes carbon balance—either positive coordination, negative coordination (a trade-off), or no coordination—should vary strongly across environments (Figure 6). Our simulations predicted that potential carbon balance can be greatest in the absence of any developmental constraint between D_s and D_t, because any constraint limits the trait space that can be explored, potentially putting the "optimum" out of reach. However, certain conditions may favor developmental constraints if D_s and D_t are strongly coordinated in a manner that maximizes carbon balance in a given environment. For example, a trade-off might be advantageous in a hot and dry environment, where trichomes are beneficial for reducing radiant load especially when a high stomatal density would not be adaptive due to scarce water. Conversely, a positive D_t–D_s association might maximize carbon balance in intermediate environments. Notably, a positive constraint may be more strongly favored after accounting for multiple additional functions of trichomes in mitigating stresses, such as reducing herbivory and shedding rain, that are often enhanced in high-productivity environments but were not included in our heuristic analysis. Disentangling the molecular, genetic, and ecological drivers across diverse species underlying the coordination or decoupling of D_t and D_s is a critical avenue for future studies, given the importance of both traits on wild and agricultural species.

The coordination of D_t and D_s has implications and applications in agriculture. Several studies in the meta-analysis found positive D_t–D_s coordination in comparisons of crop varieties. Engineering and breeding of traits that enhance biotic resistance into crops is a promising alternative to harmful chemical agents (Dong and Ronald, 2019). Additionally, plants have been bred for high D_t to confer higher herbivore deterrence and disease resistance (Pillemer and Tingey, 1976; Snyder and Antonious, 2011), and a high D_s would allow for maximized gas exchange. Yet, the carbon cost of plant defenses, including high D_t, has raised concern due to the allocation of resources away from growth or reproduction (Strauss and Agrawal, 1999). However, a high D_t coupled with high D_s may result in herbivory resistance without reducing growth or reproductive yield, which is consistent with several studies showing the lack of a growth–defense trade-off for trichomes (Agren and Schemske, 1993; Kaplan et al., 2009). Indeed, a high D_s may drive higher yield (Lu et al., 1998; Roche, 2015). A high D_t has also been suggested for increasing albedo of crops and influencing regional temperatures (Doughty et al., 2011), although much work is needed to determine the impact of this trait at the landscape scale. Toward increasing global food production to ensure global food security (Searchinger et al., 2018), future studies should further resolve the combined impacts of high D_t and D_s on crop productivity and yield and stress tolerance and examine the importance of other surface features across plant organs.

CONCLUSIONS

Our findings emphasize the power of analyzing functional traits and their associations in terms of their underlying developmental traits. We resolved the role of multiple developmental factors that underlie variation in D_t and that account for its contrasting associations with D_s in different contexts. The higher resolution of developmental causation of important functional traits provides new avenues to examine trait evolution and to breed climate-forward variants in crop species.

AUTHOR CONTRIBUTIONS

The project was conceptualized by A.S.B., C.D.M., T.N.B., and L.S. A.S.B., C.D.M., M.A.C., J.B., M.H., J.L., J.M., K.P., C.P., B.S., S.T., T.N.B., and L.S. performed data curation, and reviewed and edited the manuscript. A.S.B., T.N.B., and L.S. undertook formal analyses. C.D.M., T.N.B., and L.S. acquired funding. A.S.B., C.D.M., J.B., M.H., J.L., J.M., K.P., C.P., B.S., S.T., T.N.B., and L.S. performed the investigations. A.S.B., C.D.M., M.A.C., T.N.B., and L.S. developed the methodology. A.S.B. and L.S. administered the project. A.S.B., C.D.M., M.A.C., T.N.B., and L.S. provided resources. A.S.B. and T.N.B. wrote the software. A.S.B. and L.S. supervised the project. A.S.B., C.D.M., and L.S. validated the data. A.S.B., C.D.M., and T.N.B. provided the data visualization. A.S.B. and L.S. wrote the original draft.

DATA AVAILABILITY STATEMENT

Data are available in the online supplementary material and have also been deposited into Dryad: https://doi.org/10.5061/dryad.rv15dv4g5 (Baird, 2024).

ORCID

Alec S. Baird http://orcid.org/0000-0002-9859-5633
Camila D. Medeiros http://orcid.org/0000-0002-5822-5603
Thomas N. Buckley http://orcid.org/0000-0001-7610-7136
Lawren Sack http://orcid.org/0000-0002-7009-7202

REFERENCES

Adebooye, O. C., M. Hunsche, G. Noga, and C. Lankes. 2012. Morphology and density of trichomes and stomata of *Trichosanthes cucumerina* (Cucurbitaceae) as affected by leaf age and salinity. *Turkish Journal of Botany* 36: 328–335.

Adrian, J., J. Chang, C. E. Ballenger, B. O. R. Bargmann, J. Alassimone, K. A. Davies, O. S. Lau, et al. 2015. Transcriptome dynamics of the stomatal lineage: birth, amplification and termination of a self-renewing population. *Developmental Cell* 33: 107–118.

Agrawal, A. A., M. Fishbein, R. Jetter, J. Salminen, J. B. Goldstein, A. E. Freitag, and J. P. Sparks. 2009. Phylogenetic ecology of leaf surface traits in the milkweeds (*Asclepias* spp.): chemistry, ecophysiology, and insect behavior. *New Phytologist* 183: 848–867.

Agren, J., and D. W. Schemske. 1993. The cost of defense against herbivores: an experimental study of trichome production in *Brassica rapa*. *American Naturalist* 141: 338–350.

Azmat, R., S. Haider, H. Nasreen, F. Aziz, and M. Riaz. 2009. A viable alternative mechanism in adapting the plants to heavy metal environment. *Pakistan Journal of Botany* 41: 2729–2738.

Baird, A. 2024. Elucidating the association of trichome and stomatal densities across species [Dataset]. *Dryad*. https://doi.org/10.5061/dryad.rv15dv4g5

Barroso, A. A. M., E. Galeano, A. J. P. Albrecht, F. C. dos Reis, and R. V. Filho. 2015. Does sourgrass leaf anatomy influence glyphosate resistance? *Comunicata Scientiae* 6: 445–453.

Bickford, C. P. 2016. Ecophysiology of leaf trichomes. *Functional Plant Biology* 43: 807–814.

Brewer, C. A., W. K. Smith, and T. C. Vogelmann. 1991. Functional interaction between leaf trichomes, leaf wettability and the

optical properties of water droplets. *Plant, Cell & Environment* 14: 955–962.

Brodribb, T. J., G. J. Jordan, and R. J. Carpenter. 2013. Unified changes in cell size permit coordinated leaf evolution. *New Phytologist* 199: 559–570.

Buckley, T. N. 2005. The control of stomata by water balance. *New Phytologist* 168: 275–292.

Buckley, T. N., and A. Diaz-Espejo. 2015. Partitioning changes in photosynthetic rate into contributions from different variables. *Plant, Cell & Environment* 38: 1200–1211.

Buckley, T. N., K. A. Mott, and G. D. Farquhar. 2003. A hydromechanical and biochemical model of stomatal conductance. *Plant, Cell & Environment* 26: 1767–1785.

Cach-Pérez, M. J., J. L. Andrade, W. Cetzal-Ix, and C. Reyes-García. 2016. Environmental influence on the inter- and intraspecific variation in the density and morphology of stomata and trichomes of epiphytic bromeliads of the Yucatan Peninsula. *Botanical Journal of the Linnean Society* 181: 441–458.

Camargo, M. A. B., and R. A. Marenco. 2011. Density, size and distribution of stomata in 35 rainforest tree species in Central Amazonia. *Acta Amazonica* 41: 205–212.

Carins Murphy, M. R., G. J. Jordan, and T. J. Brodribb. 2016. Cell expansion not cell differentiation predominantly co-ordinates veins and stomata within and among herbs and woody angiosperms grown under sun and shade. *Annals of Botany* 118: 1127–1138.

Carins Murphy, M. R., G. J. Jordan, and T. J. Brodribb. 2012. Differential leaf expansion can enable hydraulic acclimation to sun and shade. *Plant, Cell & Environment* 35: 1407–1418.

Carins Murphy, M. R., G. J. Jordan, and T. J. Brodribb. 2014. Acclimation to humidity modifies the link between leaf size and the density of veins and stomata. *Plant, Cell & Environment* 37: 124–131.

Choi, Y.-E., E. Harada, M. Wada, H. Tsuboi, Y. Morita, T. Kusano, and H. Sano. 2001. Detoxification of cadmium in tobacco plants: formation and active excretion of crystals containing cadmium and calcium through trichomes. *Planta* 213: 45–50.

Choinski, J. S., and R. R. Wise. 1999. Leaf growth development in relation to gas exchange in *Quercus marilandica* Muenchh. *Journal of Plant Physiology* 154: 302–309.

Denny, M. 2017. The fallacy of the average: on the ubiquity, utility and continuing novelty of Jensen's inequality. *Journal of Experimental Biology* 220: 139–146.

Dong, O. X., and P. C. Ronald. 2019. Genetic engineering for disease resistance in plants: recent progress and future perspectives. *Plant Physiology* 180: 26–38.

Doughty, C. E., C. B. Field, and A. M. S. McMillan. 2011. Can crop albedo be increased through the modification of leaf trichomes, and could this cool regional climate? *Climatic Change* 104: 379–387.

Downs, J. L., and R. A. Black. 1999. Leaf surface characteristics and gas exchange in *Artemisia tridentata* subspecies *wyomingensis* and *tridentata*. *In* E. D. McArthur; W. K. Ostler, and C. L. Wambolt [compilers], Proceedings: shrubland ecotones, 108–112, Ephraim, UT, USA, 1998. Proceedings RMRS-P-11, U.S. Department of Agriculture, Forest Service, Rocky Mountain Research Station, Ogden, UT, USA.

Ehleringer, J. R., and O. Björkman. 1978. Pubescence and leaf spectral characteristics in a desert shrub, Encelia farinosa. *Oecologia* 36: 151–162.

Ehleringer, J., O. Björkman, and H. A. Mooney. 1976. Leaf pubescence: effects on absorptance and photosynthesis in a desert shrub. *Science* 192: 376–377.

Ehleringer, J. R., and H. A. Mooney. 1978. Leaf hairs: Effects on physiological activity and adaptive value to a desert shrub. *Oecologia* 37: 183–200.

Evert, R. F. 2006. Esau's plant anatomy: meristems, cells, and tissues of the plant body: their structure, function, and development. 3rd ed. John Wiley, Hoboken, NJ, USA.

Fambrini, M., and C. Pugliesi. 2019. The dynamic genetic–hormonal regulatory network controlling the trichome development in leaves. *Plants (Basel, Switzerland)* 8: 253.

Farquhar, G. D., S. von Caemmerer, and J. A. Berry. 1980. A biochemical model of photosynthetic CO_2 assimilation in leaves of C_3 species. *Planta* 149: 78–90.

Fernández, V., D. Sancho-Knapik, P. Guzmán, J. J. Peguero-Pina, L. Gil, G. Karabourniotis, M. Khayet, et al. 2014. Wettability, polarity, and water absorption of holm oak leaves: effect of leaf side and age. *Plant Physiology* 166: 168–180.

Franks, P. J., and D. J. Beerling. 2009. Maximum leaf conductance driven by CO_2 effects on stomatal size and density over geologic time. *Proceedings of the National Academy of Sciences, USA* 106: 10343–10347.

Fu, Q. S., R. C. Yang, H. S. Wang, B. Zhao, C. L. Zhou, S. X. Ren and Y.-D. Guo. 2013. Leaf morphological and ultrastructural performance of eggplant (Solanum melongena L.) in response to water stress. *Photosynthetica* 51: 109–114.

Galdon-Armero, J., M. Yang, H. S. Fullana-Pericas, P. A. Mulet, M. A. Conesa, C. Martin and J. Galmes. 2018. The ratio of trichomes to stomata is associated with water use efficiency in *Solanum lycopersicum* (tomato). *The Plant Journal* 96: 607–619.

Glover, B. J. 2000. Differentiation in plant epidermal cells. *Journal of Experimental Botany* 51: 497–505.

Glover, B. J., M. Perez-Rodriguez, and C. Martin. 1998. Development of several epidermal cell types can be specified by the same MYB-related plant transcription factor. *Development* 125: 3497–3508.

Grubb, P. J. 1998. A reassessment of the strategies of plants which cope with shortages of resources. *Perspectives in Plant Ecology, Evolution and Systematics* 1: 3–31.

Grubb, P. J. 1992. A positive distrust in simplicity: lessons from plant defences and from competition among plants and among animals. *Journal of Ecology* 80: 585–610.

Gudesblat, G. E., P. S. Torres, and A. A. Vojnov. 2009. Stomata and pathogens. *Plant Signaling & Behavior* 4: 1114–1116.

Gupt, S. K., R. Chand, V. K. Mishra, R. N. Ahirwar, M. Bhatta, and A. K. Joshi. 2021. Spot blotch disease of wheat as influenced by foliar trichome and stomata density. *Journal of Agriculture and Food Research* 6: 100227.

Haberlandt, G. 1914. Physiological plant anatomy, 4th ed. MacMillan, London, UK.

Handley, R., B. Ekbom, and J. Ågren. 2005. Variation in trichome density and resistance against a specialist insect herbivore in natural populations of *Arabidopsis thaliana*. *Ecological Entomology* 30: 284–292.

Hare, J. D., and E. Elle. 2002. Variable impact of diverse insect herbivores on dimorphic *Datura wrightii*. *Ecology* 83: 2711–2720.

Hetherington, A. M., and F. I. Woodward. 2003. The role of stomata in sensing and driving environmental change. *Nature* 424: 901–908.

Hoof, J., L. Sack, D. T. Webb, and E. T. Nilsen. 2008. Contrasting structure and function of pubescent and glabrous varieties of Hawaiian *Metrosideros polymorpha* (Myrtaceae) at high elevation. *Biotropica* 40: 113–118.

Huchelmann, A., M. Boutry, and C. Hachez. 2017. Plant glandular trichomes: natural cell factories of biotechnological interest. *Plant Physiology* 175: 6–22.

John, G. P., C. Scoffoni, T. N. Buckley, R. Villar, H. Poorter, and L. Sack. 2017. The anatomical and compositional basis of leaf mass per area. *Ecology Letters* 20: 412–425.

Kaplan, I., G. P. Dively, and R. F. Denno. 2009. The costs of anti-herbivore defense traits in agricultural crop plants: a case study involving leafhoppers and trichomes. *Ecological Applications* 19: 864–872.

Karabourniotis, G., and C. Fasseas. 1996. The dense indumentum with its polyphenol content may replace the protective role of the epidermis in some young xeromorphic leaves. *Canadian Journal of Botany* 74: 347–351.

Kidner, C. A., and M. C. P. Timmermans. 2010. Signaling sides adaxial–abaxial patterning in leaves. *Current Topics in Developmental Biology* 91: 141–168.

Kim, K., H. Kim, S. Ho Park, and S. Joon Lee. 2017. Hydraulic strategy of cactus trichome for absorption and storage of water under arid environment. *Frontiers in Plant Science* 8: 1777.

Konrad, W., D. L. Royer, P. J. Franks, and A. Roth-Nebelsick. 2021. Quantitative critique of leaf-based paleo-CO_2 proxies: consequences for their reliability and applicability. *Geological Journal* 56: 886–902.

Larkin, J. C., M. D. Marks, J. Nadeau, and F. Sack. 1997. Epidermal cell fate and patterning in leaves. *Plant Cell* 9: 1109–1120.

Li, C., Y. Mo, N. Wang, L. Xing, Y. Qu, Y. Chen, Z. Yuan, et al. 2023. The overlooked functions of trichomes: water absorption and metal detoxication. *Plant, Cell & Environment* 46: 669–687.

Lin, Y.-S., B. E. Medlyn, R. A. Duursma, I. C. Prentice, H. Wang, S. Baig, D. Eamus, et al. 2015. Optimal stomatal behaviour around the world. *Nature Climate Change* 5: 459–464.

Lu, Z., R. G. Percy, C. O. Qualset, and E. Zeiger. 1998. Stomatal conductance predicts yields in irrigated Pima cotton and bread wheat grown at high temperatures. *Journal of Experimental Botany* 49: 453–460.

Mauricio, R. 1998. Costs of resistance to natural enemies in field populations of the annual plant *Arabidopsis thaliana*. *American Naturalist* 151: 20–28.

Medeiros, C. D., C. Henry, S. Trueba, I. Anghel, S. D. D. de L. Guerrero, A. Pivovaroff, L. R. Fletcher, et al. 2023. Predicting plant species climate niches on the basis of mechanistic traits. *Functional Ecology* 37: 2786–2808.

Medeiros, C. D., C. Scoffoni, G. P. John, M. K. Bartlett, F. Inman-Narahari, R. Ostertag, S. Cordell, et al. 2019. An extensive suite of functional traits distinguishes Hawaiian wet and dry forests and enables prediction of species vital rates. *Functional Ecology* 33: 712–734.

Mediavilla, S., I. Martín, J. Babiano, and A. Escudero. 2019. Foliar plasticity related to gradients of heat and drought stress across crown orientations in three Mediterranean *Quercus* species. *PLoS One* 14: e0224462.

Mirzaie, M., A. R. Ladanmoghadam, L. Hakimi, and E. Danaee. 2020. Water stress modifies essential oil yield and composition, glandular trichomes and stomatal features of lemongrass (*Cymbopogon citratus*) inoculated with arbuscular mycorrhizal fungi. *Journal of Agricultural Science and Technology* 22: 1575–1585.

Muir, C. D., M. À. Conesa, J. Galmés, V. Pathare, P. Rivera, R. L. Rodríguez, T. Terrazas, and D. Xiong. 2022. How important are functional and developmental constraints on phenotypic evolution? An empirical test with the stomatal anatomy of flowering plants. *American Naturalist* 201: 794–812.

Pan, Z.-L., W. Guo, Y.-J. Zhang, J. D. M. Schreel, J.-Y. Gao, Y.-P. Li, and S.-J. Yang. 2021. Leaf trichomes of *Dendrobium* species (epiphytic orchids) in relation to foliar water uptake, leaf surface wettability, and water balance. *Environmental and Experimental Botany* 190: 104568.

Patel, I., L. Y. Gorim, K. Tanino, and A. Vandenberg. 2021. Diversity in surface microstructures of trichomes, epidermal cells, and stomata in lentil germplasm. *Frontiers in Plant Science* 12: 697692.

Pillemer, E. A., and W. M. Tingey. 1976. Hooked trichomes: A physical plant barrier to a major agricultural pest. *Science* 193: 482–484.

R Core Team. 2023. R: a language and environment for statistical computing. R Foundation for Statistical Computing, Vienna, Austria. Website: https://www.r-project.org

Rasband, W. S. 1997–2018. ImageJ. U. S. National Institutes of Health, Bethesda, Maryland, USA. Website: https://imagej.net/ij/

Ripley, B. S., N. Pammenter and V. R. Smith. 1999. Function of leaf hairs revisited: the hair layer on leaves *Arctotheca populifolia* reduces photoinhibition, but leads to higher leaf temperatures caused by lower transpiration rates. *Journal of Plant Physiology* 155: 78–85.

Roche, D. 2015. Stomatal conductance is essential for higher yield potential of C_3 crops. *Critical Reviews in Plant Sciences* 34: 429–453.

Royer, D. L. 2001. Stomatal density and stomatal index as indicators of paleoatmospheric CO_2 concentration. *Review of Palaeobotany and Palynology* 114: 1–28.

Sack, L., and T. N. Buckley. 2016. The developmental basis of stomatal density and flux. *Plant Physiology* 171: 2358–2363.

Sack, L., and T. N. Buckley. 2020. Trait multi-functionality in plant stress response. *Integrative and Comparative Biology* 60: 98–112.

Salisbury, E. 1927. I. On the causes and ecological significance of stomatal frequency, with special reference to the woodland flora. *Philosophical Transactions of the Royal Society, B, Biological Sciences* 216: 1–65.

Schreel, J. D. M., O. Leroux, W. Goossens, C. Brodersen, A. Rubinstein, and K. Steppe. 2020. Identifying the pathways for foliar water uptake in beech (*Fagus sylvatica* L.): a major role for trichomes. *Plant Journal* 103: 769–780.

Schwerbrock, R., and C. Leuschner. 2017. Foliar water uptake, a widespread phenomenon in temperate woodland ferns? *Plant Ecology* 218: 555–563.

Searchinger, T., R. Waite, C. Hanson, J. Ranganathan, and E. Matthews. 2018. Creating a sustainable food future: a menu of solutions to feed nearly 10 billion people by 2050. World Resources Institute, Washington, D.C., USA.

Serrano-Mejia, C., R. Bello-Bedoy, M. C. Arteaga and G. R. Castillo. 2022. Does domestication affect structural and functional leaf traits? A comparison between wild and cultivated Mexican chili peppers (*Capsicum annuum*). *Plants* 11: 3062.

Simon, N. M. L., J. Sugisaka, M. N. Honjo, S. A. Tunstad, G. Tunna, H. Kudoh, and A. N. Dodd. 2020. Altered stomatal patterning accompanies a trichome dimorphism in a natural population of *Arabidopsis*. *Plant Direct* 4: e00262.

Skelton, R. P., J. J. Midgley, J. M. Nyaga, S. D. Johnson, M. D. Cramer, R. P. Skelton, J. J. Midgley, et al. 2012. Is leaf pubescence of Cape Proteaceae a xeromorphic or radiation-protective trait? *Australian Journal of Botany* 60: 104–113.

Snyder, J. C., and G. F. Antonious. 2011. Trichomes – importance in plant defence and plant breeding. *CABI Reviews* 2009: 1–16.

Soheili, F., M. Heydari, S. Woodward, and H. R. Naji. 2023. Adaptive mechanism in *Quercus brantii* Lindl. leaves under climatic differentiation: morphological and anatomical traits. *Scientific Reports* 13: 3580.

Strauss, S. Y., and A. A. Agrawal. 1999. The ecology and evolution of plant tolerance to herbivory. *Trends in Ecology & Evolution* 14: 179–185.

Torii, K. U. 2021. Stomatal development in the context of epidermal tissues. *Annals of Botany* 128: 137–148.

Valverde, P. L., J. Fornoni, and J. Néñez-Farfán. 2001. Defensive role of leaf trichomes in resistance to herbivorous insects in *Datura stramonium*. *Journal of Evolutionary Biology* 14: 424–432.

Vinod, N., M. Slot, I. R. McGregor, E. M. Ordway, M. N. Smith, T. C. Taylor, L. Sack, et al. 2023. Thermal sensitivity across forest vertical profiles: patterns, mechanisms, and ecological implications. *New Phytologist* 237: 22–47.

Wang, X., C. Shen, P. Meng, G. Tan, and L. Lv. 2021. Analysis and review of trichomes in plants. *BMC Plant Biology* 21: 70.

Warton, D. I., R. A. Duursma, D. S. Falster, and S. Taskinen. 2012. smatr 3 – an R package for estimation and inference about allometric lines. *Methods in Ecology and Evolution* 3: 257–259.

Werker, E. 2000. Trichome diversity and development. *Advances in Botanical Research* 31: 1–35.

Wong, S. C., I. R. Cowan, and G. D. Farquhar. 1979. Stomatal conductance correlates with photosynthetic capacity. *Nature* 282: 424–426.

Yamaguchi, T., A. Nukazuka, and H. Tsukaya. 2012. Leaf adaxial–abaxial polarity specification and lamina outgrowth: evolution and development. *Plant and Cell Physiology* 53: 1180–1194.

Yan, L., X. Cheng, R. Jia, Q. Qin, L. Guan, H. Du, and S. Hou. 2014. New phenotypic characteristics of three tmm alleles in *Arabidopsis thaliana*. *Plant Cell Reports* 33: 719–731.

Zhu, Y., J. Zheng, H. Kang, N. Hui, S. Yin, Z. Chen, B. Du, and C. Liu. 2023. Spatial variations in leaf trichomes and their coordination with stomata in *Quercus variabilis* across Eastern Asia. *Authorea* 23 January 2003, https://doi.org/10.22541/au.167451365.50361746/v1 [preprint].

Zsögön, A. 2011. Identification and characterization of a tomato introgression line with reduced wilting under drought. Ph.D. dissertation, University of Canberra, Canberra, Australia.

SUPPORTING INFORMATION

Additional supporting information can be found online in the Supporting Information section at the end of this article.

Appendix S1. Species of diverse California angiosperm species included in the study, site(s) sampled, site latitude and longitude, site vegetation type, family, trichome morphology, trichome glandular/nonglandular, means ± SE for leaf epidermal traits measured.

Appendix S2. Details of theoretical carbon balance simulations.

Appendix S3. The intrinsic sensitivity of leaf abaxial trichome density (D_t) to developmental variables: i_s, i_t, e, s, and t.

Appendix S4. The intrinsic sensitivity of leaf abaxial stomatal density (D_s) to developmental variables: i_s, i_t, e, s, and t.

Appendix S5. The intrinsic sensitivity of leaf adaxial trichome density (D_t) to developmental variables: i_s, i_t, e, s, and t.

Appendix S6. The intrinsic sensitivity of leaf adaxial stomatal density (D_s) to developmental variables: i_s, i_t, e, s, and t.

Appendix S7. The realized sensitivity of leaf trichome density (Dt) to developmental variables: is, it, e, s, and t.